Received: 29 January 2022 | Revised: 23 May 2022 | Accepted: 25 June 2022

DOI: 10.1111/gcb.16330

Global Change Biology WILEY

RESEARCH ARTICLE

# Temperature variability interacts with mean temperature to influence the predictability of microbial phenotypes

Fei-Xue Fu[1] | Bernhard Tschitschko[2,3] | David A. Hutchins[1] | Michaela E. Larsson[2] | Kirralee G. Baker[2,4] | Allison McInnes[2,5] | Tim Kahlke[2] | Arjun Verma[2,6] | Shauna A. Murray[2,6,7] | Martina A. Doblin[2,7]

[1]Department of Biological Sciences, University of Southern California, Los Angeles, California, USA

[2]Climate Change Cluster, University of Technology Sydney, Ultimo, New South Wales, Australia

[3]Max Planck Institute for Marine Microbiology, Bremen, Germany

[4]Institute for Marine and Antarctic Studies, University of Tasmania, Hobart, Tasmania, Australia

[5]Centre for Microbiome Research, School of Biomedical Sciences, Translational Research Institute, Queensland University of Technology, Woolloongabba, Queensland, Australia

[6]School of Life Sciences, University of Technology Sydney, Ultimo, New South Wales, Australia

[7]Sydney Institute of Marine Science, Mosman, New South Wales, Australia

**Correspondence**
Martina A. Doblin, Climate Change Cluster, University of Technology Sydney, PO Box 123 Broadway, Ultimo, NSW 2007, Australia.
Email: martina.doblin@uts.edu.au

**Funding information**
Australian Research Council, Grant/Award Number: DP140101340 and DP180100054; University of Technology Sydney Distinguished Visiting Professor Scheme; U.S. National Science Foundation, Grant/Award Number: OCE 1851222 and OCE 1638804; University of Technology Sydney

## Abstract

Despite their relatively high thermal optima ($T_{opt}$), tropical taxa may be particularly vulnerable to a rising baseline and increased temperature variation because they live in relatively stable temperatures closer to their $T_{opt}$. We examined how microbial eukaryotes with differing thermal histories responded to temperature fluctuations of different amplitudes (0 control, ±2, ±4°C) around mean temperatures below or above their $T_{opt}$. Cosmopolitan dinoflagellates were selected based on their distinct thermal traits and included two species of the same genus (tropical and temperate *Coolia* spp.), and two strains of the same species maintained at different temperatures for >500 generations (tropical *Amphidinium massartii* control temperature and high temperature, CT and HT, respectively). There was a universal decline in population growth rate under temperature fluctuations, but strains with narrower thermal niche breadth (temperate *Coolia* and HT) showed ~10% greater reduction in growth. At suboptimal mean temperatures, cells in the cool phase of the fluctuation stopped dividing, fixed less carbon (C) and had enlarged cell volumes that scaled positively with elemental C, N, and P and C:Chlorophyll-*a*. However, at a supra-optimal mean temperature, fixed C was directed away from cell division and novel trait combinations developed, leading to greater phenotypic diversity. At the molecular level, heat-shock proteins, and chaperones, in addition to transcripts involving genome rearrangements, were upregulated in CT and HT during the warm phase of the supra-optimal fluctuation (30 ± 4°C), a stress response indicating protection. In contrast, the tropical *Coolia* species upregulated major energy pathways in the warm phase of its supra-optimal fluctuation (25 ± 4°C), indicating a broadscale shift in metabolism. Our results demonstrate divergent effects between taxa and that temporal variability in environmental conditions interacts with changes in the thermal mean to mediate microbial responses to global change, with implications for biogeochemical cycling.

Fu and Tschitschko should be considered joint first author.

KEYWORDS
climate impact, climate variability, dinoflagellate, primary productivity

## 1 | INTRODUCTION

The ocean has absorbed 50% of the carbon dioxide ($CO_2$) emitted through anthropogenic activity in the Earth's biosphere and >90% of the heat trapped at the Earth's surface (Domingues et al., 2008). As a result, the global ocean has warmed at an average rate of ~0.062 ± 0.013°C per decade from 1900 to 2019 (Garcia-Soto et al., 2021), and depending on the $CO_2$ emissions scenario, it is anticipated surface waters will warm by at least twice that rate by 2100 under a low warming scenario (SSP1-2.6) or by 4–8 times under a high warming scenario (SSP5-8.5) (Arias et al., 2021). In addition to long-term warming, the ocean has also experienced more frequent and intense marine heatwaves (anomalous warming events) over the last century (Oliver et al., 2018), with this trend projected to increase further under climate change (Frölicher et al., 2018).

The biological implications of a shifting baseline as well as increasing environmental variation are unknown (Kroeker et al., 2020). Our present understanding of the future distribution of species is based on climate-envelope or ecological niche models, which forecast the availability of suitable environments for different taxa that are defined by their traits (Araújo et al., 2005; Dutkiewicz et al., 2013). The values of these traits are developed from field-based observations and meta-analyses that are largely derived from cultivation experiments under constant conditions (Dutkiewicz et al., 2015; Eppley, 1972). Although we are beginning to quantify the impacts of environmental variation compared with a change in mean condition (Cabrerizo et al., 2021; Gill et al., 2022; Pansch & Hiebenthal, 2019), such trait models have largely ignored the biological processes that influence species persistence under more variable conditions, and currently do not allow for organisms to dynamically respond to their environment.

Currently, it is unclear how selection for higher thermal optima ($T_{opt}$) in response to ocean warming (i.e., increases in mean temperature) will affect species' capacities to adapt to changes in thermal variation. Plasticity, the phenotypic variation arising from the interaction of genotypes with their environment, is widely acknowledged as an important response to environmental change (Schlichting & Pigliucci, 1998). Theory predicts that plasticity should evolve in highly predictable environments, whereas reduced plasticity is expected in environments that fluctuate less predictably, because this lowers the risk that physiological responses do not match future selective pressures (Botero et al., 2015; Lande, 2009; Leung et al., 2020). There are a range of molecular, morphological, and physiological traits that are responsive to temperature, including body size (Daufresne et al., 2009), intracellular composition (Woods et al., 2003), the ratio of RNA to protein (Toseland et al., 2013), the use of heat-shock proteins (HSPs) (Feder & Hofmann, 1999), and for photosynthetic microbes, photochemistry, carbon fixation and respiration, as well as changes in photosynthetic pigments and proteins like Rubisco (Baker et al., 2016; Schaum et al., 2018; Valentin & Mock, 2004). Temperature variability in marine environments shows a broad-scale latitudinal pattern, with minimal seasonality in tropical environments and maximal in the temperate mid-latitudes (Doblin & van Sebille, 2016; Locarnini et al., 2018). It follows that tropical species with highest $T_{opt}$ for growth and physiological functions have reduced tolerance to temperature variation due to their evolution under relatively stable temperatures (Qu et al., 2019; Thomas et al., 2012). Furthermore, the shape of thermal performance curves (TPC) means that fluctuations on the ascending portion of the TPC would lead to an acceleration in growth (*Response A*; see Figure 2), whereas fluctuations on the descending portion would cause a deceleration in growth (*Response D*) (Bernhardt et al., 2018).

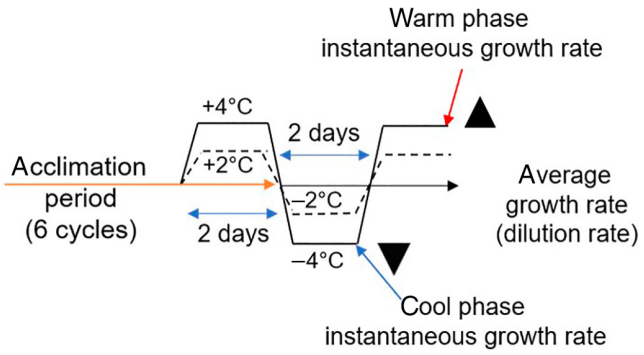


**FIGURE 1** Design of temperature treatments. Temperatures fluctuated regularly every 2 days around a mean throughout an initial acclimation period involving six growth cycles (20–28 days). Cells were then harvested under the final downward (cool) and upward (warm) phase to quantify phenotypic traits.

Here, we explicitly test how temperature variability interacts with mean temperature to influence growth and phenotypic plasticity among cosmopolitan tropical and temperate eukaryotic microbes. We used two species of the same genus, and two strains of the same species, each with a different thermal history, to investigate how universal their responses were. Strains included the potentially harmful dinoflagellate *Coolia palmyrensis* and *Coolia malayensis* with similar thermal traits ($T_{opt}$, niche breadth) even though they were isolated from tropical and temperate latitudes, respectively (Larsson et al., 2019), and two strains of the tropical dinoflagellate *Amphidinium massartii* with different thermal traits; one that was maintained at the standard growth temperature of 25°C (referred to as the control strain [CT]) and another that had undergone directional high-temperature selection at +5°C for 3.25 years (>500 generations) (referred to as the high-temperature strain [HT]) (Baker et al., 2018). Temperature treatments were designed to fluctuate with a period of 2 days at different amplitudes (0 control, ±2, ±4°C)

around different means (20, 25, 30°C) that were below or above the estimated $T_{opt}$ of each strain (Figure 1; Table S1). Exposure to regular temperature fluctuations led to a universal reduction in average population growth rate, but there was a greater cost to growth for temperate *C. malayensis* and *A. massartii* HT (strains with narrower thermal niche breadth). At suboptimal mean temperature, traits were linearly correlated to cell volume. However, at supra-optimal mean temperature, novel trait combinations developed, leading to greater phenotypic heterogeneity. Furthermore, growth declined as expected in the warm phase but also declined during the cool phase of fluctuations, indicating that the TPC does not reliably predict performance at supra-optimal mean temperature. Together, these empirical data show that phenotypic traits become less predictable at mean temperatures above $T_{opt}$ and thermal specialisation (narrower niche breadth) may come at the expense of lowered tolerance to temperature variability.

## 2 | MATERIALS AND METHODS

### 2.1 | Microbial eukaryote taxa and temperature selection environments

Experiments were performed using dinoflagellates isolated from tropical and temperate latitudes (Table S1). Tropical *A. massartii* (CS-259) was provided by S. Murray after it was isolated from Kurrimine Beach and described in Murray et al. (2012). It was grown under temperature selection for 39 months at two different temperatures (25 and 30°C; CT and HT, respectively), after which the HT strain had become high-temperature specialized, with a +2.67°C shift in the $T_{opt}$ and a +14.92°C increase in the $T_{min}$, with the overall effect of narrowing the thermal niche (Baker et al., 2018). A second tropical dinoflagellate *C. palmyrensis* and a temperate dinoflagellate *Coolia malayensis* isolated within months of each other in 2014 (Larsson et al., 2019) were also used, allowing us to examine whether thermal history influences responses of strains to thermally variable environments.

*A. massartii* was cultivated in coastal seawater medium with modified *f*/2 enrichment, lacking silicic acid (Guillard & Ryther, 1962). *Coolia* spp. was cultivated in coastal seawater medium with modified K nutrients (Litaker et al., 2009). All cultures were maintained under a light intensity of 100 µmol photons $m^{-2}$ $s^{-1}$ with a light–dark cycle of 12:12 light: dark (LD) in either 25°C (CT, *Coolia* spp.) or 30°C (HT).

### 2.2 | Experimental setup

Thermal regimes were designed to test the effect of regular thermal fluctuations in comparison with stable control treatments with the same mean temperature. Control treatments had thermal variability of <0.1°C over the experimental duration. The amplitude of temperature fluctuations was ±2 or ±4°C with temperatures in the variable treatments cycling every 2 days between temperature endpoints (Figure 1). Similar frequencies of short-term temperature variations are observed in coastal waters worldwide (Aguirre et al., 2021; Dai et al., 2009; Leinweber et al., 2009; Shaw et al., 2012). Such temperature variations are especially pronounced in coastal regimes due to the effects of atmospheric weather fluctuations on a shallow water column along with vigorous advection, mixing and upwelling (Aguirre et al., 2021; Leinweber et al., 2009). Mean temperatures for experiments were determined based on two considerations: (1) seasonal sea surface temperatures in tropical eastern Australian waters (AIMS, 2009): 20°C (winter; July) and 30°C (summer; January) and (2) the long-term culturing temperature of isolates (Table S1). For CT ad HT strains, this equated to reciprocal temperature transplants at 25 and 30°C.

To determine the effect of amplitude in variable thermal regimes, all taxa were exposed to 25 ± 2 and ±4°C, relative to the stable control—that is, temperature varied from 23°C to 27°C or from 21 to 29°C (Table S2). To examine the effect of thermal variation centered around different mean temperatures, *A. massartii* CT and HT strains were exposed to 30 ± 4°C (26 to 34°C), and *C. palmyrensis* and *C. malayensis* were exposed to 20 ± 4°C (16 to 24°C; Table S2). Given the TPC of *Coolia* spp., fluctuations around 20°C were below $T_{opt}$ and fluctuations around 25°C were supra-optimal; for *Amphidinium*, fluctuations around 25°C were around $T_{opt}$, and those around 30°C were supra-optimal.

Experiments were conducted in a temperature-controlled room, where a system of water baths was used to maintain incubation temperatures. Temperatures in the variable treatments were adjusted every 2 days using thermostatically controlled cooling and heating systems (Julabo GmbH), with temperature shifts occurring over 60 min. Experimental microcosms consisted of 500 ml capped polycarbonate flasks filled with 400 ml of culture, illuminated from above with LED light banks (Schenzen Cidly Group) at 150 µmol photons $m^{-2}$ $s^{-1}$ in a 12:12 light: dark cycle.

Semi-continuous dilution culturing methods were used to acclimate cells to variable temperature treatments (Figure S2) and avoid excessive biomass accumulation and consequent nutrient limitation or self-shading. At the end of every dilution cycle, each bottle was diluted individually back to the initial cell concentration for that bottle. Thus, in this semi-continuous "turbidostat" method, the growth rate in each treatment determined the dilution rate. After 6 cycles (~32 days), cells were subsampled for physiological trait quantification at the end of the 2-day cool exposure period (downward phase) and then 2 days later, at the end of the warm exposure period (upward phase) (Figure 1). All experiments used three replicate bottles in each treatment.

### 2.3 | Trait quantification

#### 2.3.1 | Biomass, relative cell size estimates, and specific growth rates

Biomass was estimated every second day using in vivo chlorophyll-*a* (Chl-*a*) fluorescence to determine semi-continuous dilution volumes

based on calculated specific growth rates. These in vivo Chl-*a* estimates were later validated with microscopic or flow cytometric cell counts; growth rates calculated with these two methods were found to be closely comparable.

Cell abundance of *A. massartii* was determined with flow cytometry. One mL of culture was first fixed in paraformaldehyde solution (1% v/v final concentration), snap frozen in liquid nitrogen and stored at −80°C. Prior to enumeration, samples were thawed quickly in a 35°C water bath, vortexed and analysed with an Influx flow cytometer (BD Biosciences) under blue (488 nm laser) excitation. Yellow-green fluorescent beads were added in known concentrations for volumetric and fluorometric internal calibration. Events were triggered on FSC for enhanced sensitivity; populations were isolated on cytograms of FSC and chlorophyll-*a* fluorescence (692/40 nm). Cell count samples for the *Coolia* experiments were preserved in Lugols (1% final solution) and were then enumerated under the microscope using a Sedgewick Rafter Chamber.

### 2.3.2 | Cell size

*A. massartii* cell size was estimated using flow cytometric forward scatter, relative to bead standards (Marie et al., 1999). For *Coolia* spp., Lugols-preserved subsamples were aliquoted into 24-well glass bottom plates, and cells were measured with an automated imaging system (IN CELL 2200, GE Healthcare) using a 20× objective. Images were analysed with proprietary software to obtain major axis length, minor axis length and form factor (i.e., cell roundness, varying between 0 and 1 with 1 being a perfect circle). Biovolume was calculated based on an ellipsoid shape using minor axis as width and major axis as length, according to Hillebrand et al. (1999).

### 2.3.3 | Chlorophyll and elemental composition

Chlorophyll-*a* samples were extracted using 90% acetone for 24 h in a −20°C freezer in the dark and measured on a calibrated fluorometer (Turner designs Model 10 AU) (Fu et al., 2005). Particulate organic carbon, nitrogen and phosphorus (POC, PON, and POP, respectively) samples were filtered onto pre-combusted GF/F filters and dried at 60°C, then stored at room temperature. PON and POC was measured using an elemental combustion system (Model 4010, Costech) (Hutchins et al., 1998). POP samples were combusted at high temperature (500°C) to convert the organic P into orthophosphate, and then measurements were performed using the standard colorimetric molybdate method (Strickland & Parsons, 1968).

### 2.3.4 | Primary productivity ($^{14}$C uptake)

To estimate primary productivity, carbon fixation rates were measured using $^{14}$C-labeled bicarbonate in small volume incubations as described in Doblin et al. (2011). Specifically, radiolabelled $NaH^{14}CO_3$ (stock solution $1.85 \times 10^7$ Bq) was added to 5 ml of culture in clear glass tubes (1.5 μCi per tube) and incubated at the treatment temperature for 60–80 min under the growth irradiance. Activity in the samples was determined by removing a 100 μL aliquot and placing it into 5 ml of refrigerated 0.1 M NaOH, adding 10 ml scintillation fluid (Ultima Gold™, PerkinElmer) and shaking before counting using a liquid scintillation counter (Packard TriCarb 2900TR). Following incubation, tube contents were acidified with 250 μl 6 M HCl and shaken on an orbital shaker for 12 h to remove unfixed $^{14}$C. Scintillation fluid (10 ml Ultima Gold, Perkin Elmer) was then added to each sample, vigorously shaken and left for 1 h before counting. Counting time was set to 5 min so that counts were within a 5% counting error.

## 2.4 | RNA sampling, extraction, and analysis

Cells were sampled between hour 1 and 2 of the light period to limit diel effects, and immediately filtered onto 5 μm 25-mm polycarbonate membranes before being flash frozen in LN2 and stored at −80°C. Due to resource limitations, only control and ±4°C fluctuation samples from CT, HT, and *C. palmyrensis* were analysed further (Table S2). RNA extraction was performed based on methods described in Verma et al. (2019). Briefly, preheated Trireagent (Ambion) and bead beating was used for cell lysis. RNA was purified using RNeasy Mini Kit (Qiagen) according to manufacturer's instructions. Any residual DNA was removed via the TURBO DNA-free™ Kit (Life Technologies) according to manufacturer's instructions and RNA was then stored at −80°C. The RNA purity, quantity, and integrity were assessed using a Nanodrop ND-1000 (Thermo Scientific) and 2100 Bioanalyser Nano and Pico chips (Agilent Technologies) depending on RNA yields.

Following RNA extractions, sequencing libraries were prepared for 2–3 replicates per sample using the Illumina TruSeq stranded mRNA sample prep following the manufacturer's instructions in two batches. The first batch comprised all libraries from Amphidinium 30 ± 4°C samples. Those samples yielded relatively low RNA quantities (on average 491 ng), hence the libraries were prepared using a higher number of PCR cycles (15 cycles). The second batch comprised the libraries from all remaining samples, prepared using 12 PCR cycles. All libraries (71) were sequenced together using one Illumina NovaSeq S1 flow cell (paired-end, 2 × 100 bp reads) yielding 23 to 58 million read pairs per sample (30 million on average). Raw sequencing data has been deposited to the NCBI Sequence Read Archive under Bioproject PRJNA819215.

## 2.5 | Quality trimming, assembly, clustering, differential expression analysis

Sequencing reads were quality trimmed using trimmomatics (Bolger et al., 2014), using the default settings (ILLUMINACLIP:$TRIMMOMATIC_DIR/adapters/TruSeq3-PE.fa:2:30:10 SLIDINGWINDOW:4:5 LEADING:5

TRAILING:5 MINLEN:25). Quality trimmed reads were assembled into transcripts using Trinity version 2.6.6 (Grabherr et al., 2011; Haas et al., 2013). For *C. palmyrensis*, reads from all samples and replicates were used to generate one combined assembly. Similarly, for *A. massartii*, because both strains originate from the same clonal culture, reads from all samples and replicates from the CT and HT strains were used to generate one combined *Amphidinium* assembly. In each assembly, similar transcripts were clustered and only the longest transcript retained using CD-HIT-EST (word size of 8 and sequence identity threshold of 0.9) (Weizhong & Adam, 2006). Transcriptome completeness was estimated using BUSCO (version 3.0.2) and the eukaryote database of conserved single copy genes (eykaryota_odb9, creation date: 2016-11-02) (Simão et al., 2015).

Transcript abundance was calculated using kallisto (Bray et al., 2016) within the Trinity package. Differential expression analysis was done using edgeR (Robinson et al., 2010) within the Trinity package and was performed separately for each species and experiment, using a false discovery rate (FDR) of <0.05 and a minimum twofold change in abundance. To identify differentially expressed transcripts between the variable and the stable control treatments, differential expression analysis was performed on each sample of the variable treatments against both samples from the respective control treatment; only transcripts that were significantly DE in comparison with both control samples were considered DE between variable and control treatment.

Functional annotation of transcripts, including Gene Ontology (GO) annotation, was done using Blast2GO version 5.2.5 (Gotz et al., 2008) based on BLASTX searches against the NCBI non-redundant protein database (nr) (standalone BLAST+ version 2.7.1 [Camacho et al., 2009]) and InterProScan searches (version 5.30-69 [Jones et al., 2014]). Annotation of photosynthesis and stress-related transcripts was manually confirmed. Enrichment testing of biological process (BP) GO categories within sets of differentially expressed transcripts was done within Blast2GO using Fisher's exact test with a FDR of 0.05, corrected for multiple hypothesis testing (Benjamini & Yosef, 1995). Enriched BP GO categories were further reduced to only the most specific terms (more general GO terms on higher levels in the Directed Acyclic Graph [DAG] were removed).

## 2.6 | Statistical treatment of data

Statistical analyses were performed using IBM SPSS Statistics 24. Prior to analysis data was checked for normality and homoscedasticity. Data were analyzed by ANOVA using strain, mean temperature, and amplitude as fixed factors. Differences in multi-variate phenotypes were tested using ANOSIM (PRIMER-E v.6). Draftsman plots were used to visualise correlations among traits before the similarity matrix using Bray-Curtis distance was constructed.

**TABLE 1** Growth rates (mean ± SD; $day^{-1}$) for four dinoflagellate strains grown at different mean temperatures with different amplitude of regular (2-day) temperature fluctuations ($n = 3$)

| | 20°C mean | 20°C mean | 25°C mean | 25°C mean | 25°C mean | 30°C mean | 30°C mean |
|---|---|---|---|---|---|---|---|
| | Stable control | ±4°C | Stable control | ±2°C | ±4°C | Stable control | ±4°C |
| *Amphidinium massartii* CT | | | $0.630 \pm 0.019^{a}$ | $0.540 \pm 0.010^{ab}$ | $0.513 \pm 0.059^{b}$ | $0.686 \pm 0.016$ | $0.199 \pm 0.012^{*}$ |
| *A. massartii* HT | | | $0.527 \pm 0.027^{a}$ | $0.420 \pm 0.009^{b}$ | $0.364 \pm 0.018^{c}$ | $0.557 \pm 0.027$ | $0.107 \pm 0.015^{*}$ |
| *Coolia palmyrensis* tropical | $0.264 \pm 0.010$ | $0.197 \pm 0.007^{*}$ | $0.412 \pm 0.008^{a}$ | $0.370 \pm 0.005^{b}$ | $0.346 \pm 0.012^{c}$ | | |
| *C. malayensis* temperate | $0.245 \pm 0.002$ | $0.163 \pm 0.017^{*}$ | $0.359 \pm 0.012^{a}$ | $0.269 \pm 0.008^{b}$ | $0.295 \pm 0.032^{b}$ | | |

*Note:* Asterisks show that growth rates under fluctuating temperature are significantly lower than those at stable temperature (ANOVA, $p < .05$), with letter superscripts indicating differences among different amplitudes at a mean temperature of 25°C.

## 3 | RESULTS

### 3.1 | Effects on growth

Following an acclimation period (Figure 1 and Figure S2), average population growth rate under fluctuating conditions was significantly lower than under stable conditions in all four dinoflagellate strains (Table 1; ANOVA Type III, $F_{[1,23]}$ 23.93, $p < .001$), irrespective of mean temperature. Thermal variability caused the greatest negative impact (>70% decline) to both the HT and CT strains of *A. massartii* when the temperature fluctuated ±4°C around the supra-optimal (30°C) compared with the standard mean (25°C) (ANOVA Type III, $F_{(2,22)} = 132.561$, $p < .001$). The amplitude (±2 vs. ±4°C) of the temperature fluctuation (tested at 25°C for all taxa; see Section 2 and Table S2) was significant for *A. massartii* HT (ANOVA type III, $F_{[2,6]} = 54.349$, $p < .001$) and tropical *C. palmyrensis* (ANOVA Type III, $F_{[2,6]} = 40.776$, $p < .001$; Table 1), both showing a greater decline in the average population growth with increasing amplitude. However, the decline in growth was similar in the ±2 and ±4°C fluctuations for *A. massartii* CT and the temperate *C. malayensis* population, which may be due to larger between replicate differences.

Growth of all strains responded dynamically to within treatment temperature changes, with instantaneous growth rates diverging at temperature fluctuation endpoints (i.e., cool/downward and warm/upward phases; Figure 2). Reduced growth during downward fluctuations and increased growth during upward fluctuations (with intermediate growth under stable mean temperature) was anticipated at mean temperatures below $T_{opt}$ in the ascending portion of the TPC (Bernhardt et al., 2018). This response was termed *Response A* (Figure 2). In contrast, *Response D* occurred at mean temperatures above $T_{opt}$ in the descending portion of the TPC and was characterised by reductions in growth rate under both upward and downward temperature fluctuations relative to the stable temperature treatment, indicating that cells were redirecting resources away from cell division (Figure 2).

The average population growth rate of *Coolia* species under fluctuating temperatures was less impacted than *Amphidinium* (Figure 2; Table 1), likely due to longer generational times (2.6 days in *Coolia* spp. vs. 1.7 days in *Amphidinium*: Table 1) that exceeded the 2-day frequency of fluctuations. At the mean temperature of 20°C (3.6 to 4.5°C below $T_{opt}$; Table S1), instantaneous growth rates of *Coolia* spp. under ±4°C fluctuations diminished by −96.0% ± 10.5% (mean ± SD; tropical *C. palmyrensis*) and −110.4% ± 1.2% (temperate *C. malayensis*) relative to stable controls in the downwards phase of the fluctuation (16°C) and increased to 64.8% ± 18.3% and 43.6% ± 13.2% in the upwards phase (24°C)—that is, the growth dynamics of both species were characteristic of *Response A* (Figure 2). However, under ±4°C temperature fluctuations at the mean temperature of

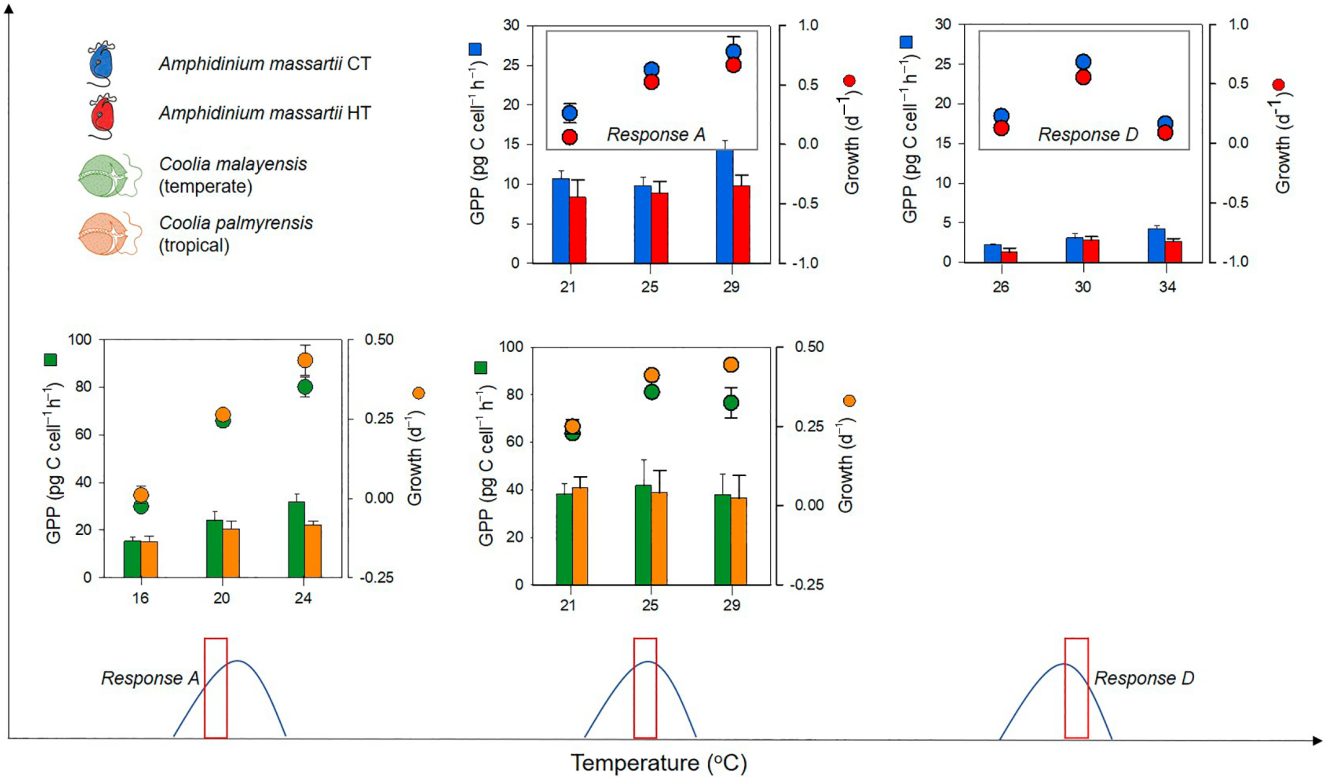


FIGURE 2 Impact of temperature fluctuations on microbial eukaryotes. Carbon biomass normalised GPP (mean ± SD) and instantaneous growth rates (mean) of dinoflagellate strains in the downwards and upwards phase of fluctuating temperature treatments compared with growth in the stable control ($n = 3$). *Response A* is characterised by growth in the downward/upward phase being lower/higher than control (mean) temperature. *Response D* is characterised by growth in both the downward and upward phase being lower than the stable control. Note different *x*-axis scales between plots.

25°C (0.5–1.4°C above $T_{opt}$; Table S1), the tropical *C. palmyrensis* strain exhibited *Response A* (instantaneous growth rates declined by −39.4% ± 5.6% at 21°C and increased by +8.1% ± 1.2% at 29°C) whereas the temperate *C. malayensis* showed *Response D*, characterised by a reduction in instantaneous growth in both the downwards (−36.3% ± 0.2%) and upwards phases (−9.4% ± 13.3%) of the 25 ± 4°C fluctuation relative to stable controls (Figure 2).

Both strains of *A. massartii* exhibited similar growth patterns under thermal fluctuations. At the mean temperature of 25°C with ±4°C fluctuation, CT and HT exhibited *Response A*. Growth of the CT strain ($T_{opt}$ 23.94°C) declined by −58.4% ± 12.7% in the downwards phase (21°C) and increased by 24.1% ± 19.9% in the upwards phase (29°C) relative to stable controls (Figure 2). The HT strain ($T_{opt}$ 26.61°C) showed an even greater decline in growth at 21°C in the downwards phase (−88.4% ± 4.1%) compared with the CT strain (Figure 2), and a similar increase in growth (+27.0% ± 2.7%) at 29°C in the upwards phase. At mean temperature of 30°C (+3.39 to 6.06°C above $T_{opt}$ for both strains; Table S1), both CT and HT exhibited *Response D* but the decline in growth was 10% greater in the HT compared with the CT strain (−76.7% ± 5.5% vs. −66.4% ± 3.9% at 26°C and −83.7% ± 3.2% vs. −75.6% ± 1.7% at 34°C, respectively; ANOVA $F_{[1,9]} = 14.508$, $p = .004$), resulting in a significantly lower overall HT growth rate (Figure 2; Table 1).

## 3.2 | Effects on phenotypic traits

There were significant trait value changes between the downward and upward phases of the fluctuations, indicating phenotypic plasticity of all strains (Data Table). As part of *Response A*, cell volume was directly proportional to growth (Figure 3; Table S3), most clearly illustrated by the tropical *C. palmyrensis* in the 20 ± 4°C treatment. When temperatures approached 16°C, growth slowed (i.e., cell division ceased), and cell volume was maximal, as was elemental carbon (C), nitrogen (N), and phosphorus (P) content. Conversely, as temperatures approached 24°C, growth increased, and cell volume diminished alongside cellular C, N, and P. Cellular chlorophyll-*a* (Chl-a) content and gross primary productivity (GPP; carbon fixation measured over 1–2 h) showed poor correspondence to cell volume, but C:Chl-a was positively correlated. The same pattern was observed for both *Amphidinium* strains when temperatures fluctuated around 25°C (Figure 3).

*Response D* however, characterised by relatively low growth rates at the downward and upward phases of temperature fluctuations around a supra-optimal mean, led to new trait combinations that were most apparent in *Amphidinium* (Figure 4). In the 30 ± 4°C regime, *A. massartii* cells became significantly larger but a distinct elemental composition was evident for the HT strain which had higher N per biomass and hence lower C:N compared with the CT population (Figure 4). In the 25 ± 4°C treatment close to $T_{opt}$, *Amphidinium* cells were smallest, most pigmented and had maximal rates of carbon fixation (GPP; gross primary production). *Amphidinium* phenotypes diverged between stable and fluctuating treatments (ANOSIM Global $R = .330$, $p = .001$), at specific temperatures (ANOSIM Global $R = .788$, $p = .001$) except for 25 and 29°C (pairwise tests) as well as between CT and HT strains (ANOSIM Global $R = .117$, $p = .019$). *Coolia* phenotypes appeared less plastic to the imposed thermal treatments (Figure 4), with tropical and temperate species responding similarly (ANOSIM, $R = .056$ $p = .113$) with phenotypes only distinct between different temperatures (Figure S5; ANOSIM Global $R = .678$, $p = .001$).

## 3.3 | Effects on metabolism

To help uncover how changes in the temperature environment impacted different strains, we examined carbon fixation (i.e., GPP) in relation to growth rates as well as gene expression at downward and upward phases relative to stable mean temperature controls. In *Coolia* spp., GPP (normalised to carbon biomass) was proportional to growth at 20 ± 4°C, increasing with growth rate in the upward phase, and decreasing with growth rate in the downward

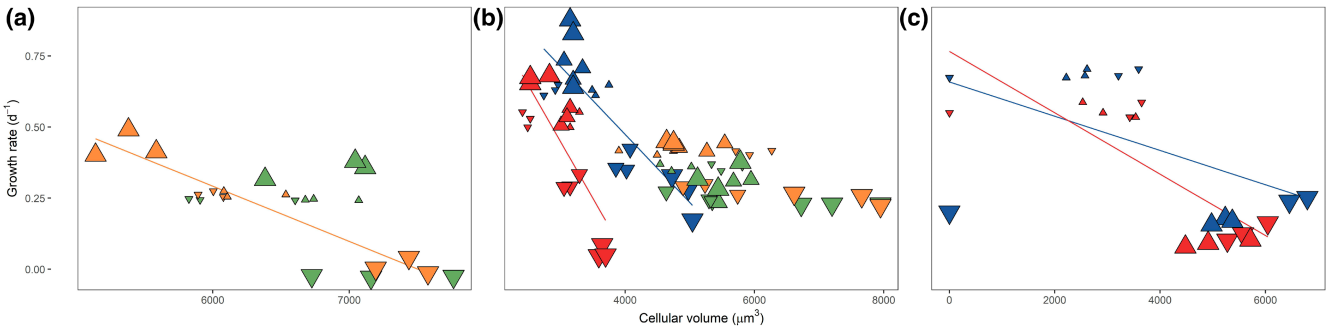


FIGURE 3 Cell volume–dependent growth. Temperate and tropical *Coolia* spp. strains (green and orange symbols, respectively) at 20°C (a), all strains at 25°C (b) and *Amphidinium massartii* control temperature and high-temperature strains (blue and red symbols, respectively) at 30°C (c). Lines reflect significant linear regression ($p < .05$). Size of symbol reflects magnitude of fluctuation amplitude, whereby largest symbols are ±4°C treatments, smallest symbols are stable treatments and intermediate symbols are ±2°C treatments. Upward and downward facing symbols depict warm and cool phases of temperature fluctuation treatments, respectively. Each symbol represents a distinct biological replicate.

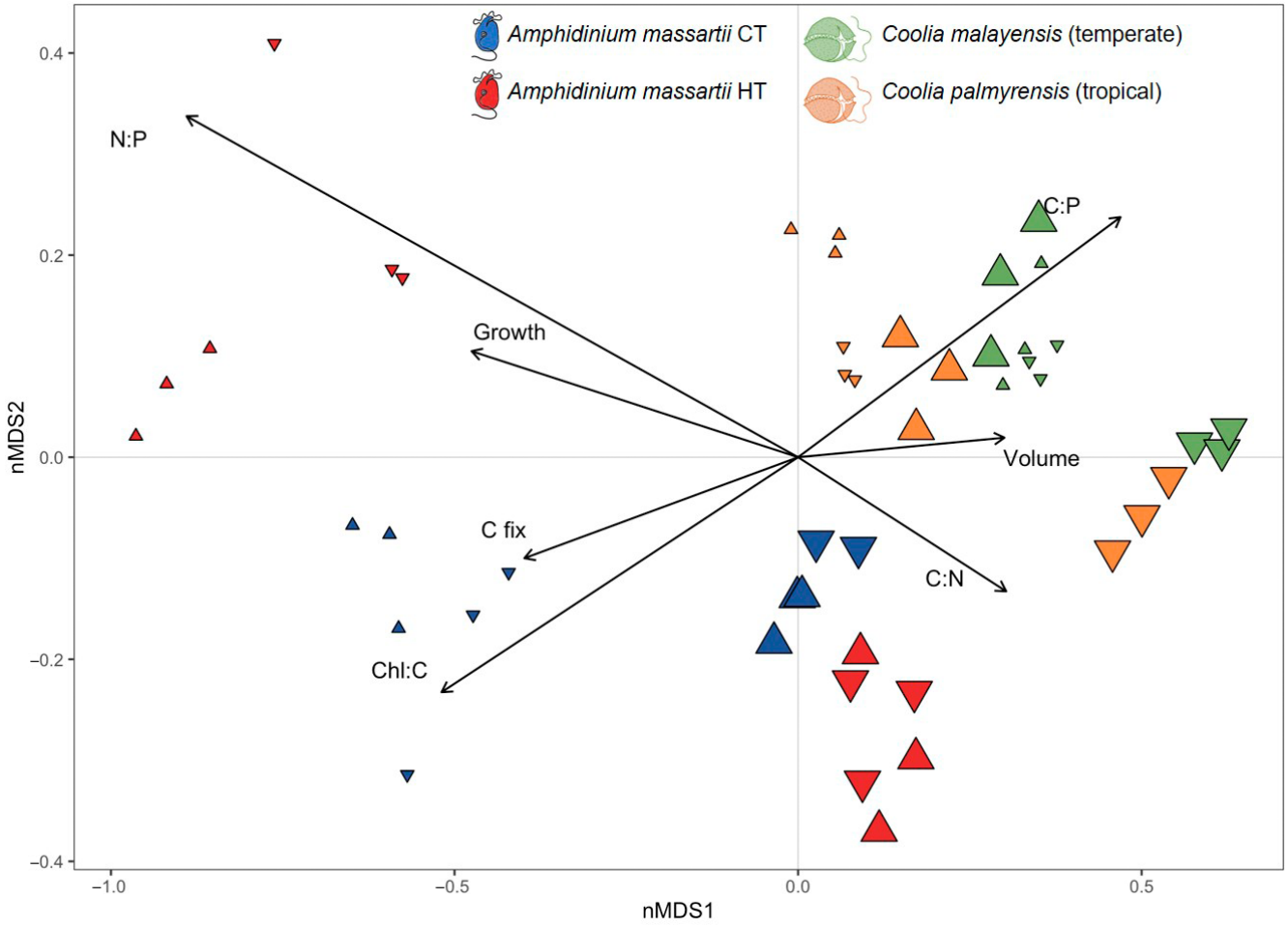


**FIGURE 4** Viable multitrait phenotypes of *Coolia* spp. and *Amphidinium massartii*. Resultant trait combinations in control and fluctuating temperature centred around a mean of 20°C (*Coolia*) and 30°C (*Amphidinium*). nMDS input variables include growth, cell size, cellular carbon, nitrogen, phosphorus content, C:N, N:P, chlorophyll-*a* content, and gross primary productivity. Vectors show the traits driving differences between phenotypes (Pearson correlation >0.7). Symbols represent tropical *Coolia palmyrensis* (orange) temperate *Coolia malayensis* (green), *A. massartii* CT (blue) and HT (red) strains. Symbol directions (upward or downward) and size are the same as Figure 3.

phase of fluctuations (Figure 2). However, when temperature fluctuated at 25 ± 4°C, GPP was a factor of ~2 higher and remained relatively constant in both downward and upward phases, with instantaneous growth rates that were similar to the 20 ± 4°C treatment (Figure 2). The pattern was similar in *Amphidinium*, but because growth did not increase in the downward phase at supra-optimal mean temperature (Figure 2; Table 1) we interpret this to mean that fixed carbon was being directed away from cell division. Notably, biomass normalised carbon fixation rates were lower in the HT versus CT strain except in stable temperature controls (Figure 2).

In *Coolia* spp., growth rates were lowest in the downward phase of fluctuations at mean temperatures of both 20 and 25°C for both the tropical and temperate strains (Figure 2). Even though the tropical *C. palmyrensis* strain grew extremely slowly at 16°C (downward phase of 20 ± 4°C) (0.011 ± 0.028 $day^{-1}$; ~97% slower than its maximum), there was relatively little downregulation of gene expression (Figure S1). In comparison, a wide range of transcripts encoding photosynthetic functions were upregulated at both 21 and 29°C (25 ± 4°C), consistent with higher carbon fixation rates than in the 20 ± 4°C regime (Figure S3). When exposed to 29°C (upward phase of 25 ± 4°C), instantaneous growth rates of *C. palmyrensis* were faster than in the stable mean control temperature of 25°C (0.445 ± 0.005 $day^{-1}$ vs. 0.412 ± 0.008 $day^{-1}$, respectively) and were accompanied by large transcriptional changes (Figure S1). Although the number of downregulated transcripts was large, many of them could not be annotated and thus encoded for unknown functions. In contrast, 43 BP GO categories for various metabolic functions were enriched in the upregulated transcripts (Figure S4), including 28 transcripts involving photosynthesis functions (Figure S3B), indicative of a broad-scale shift in metabolism.

In general, more transcripts were differentially expressed in the *A. massartii* HT strain than the CT strain in both the 25 ± 4°C and 30 ± 4°C regimes, suggesting it was undergoing more physiological adjustments (Figure S1). At 21°C (downward phase of 25 ± 4°C), the HT strain had a considerably slower growth rate at 0.061 ± 0.022 $day^{-1}$ (~90% slower than its maximum) relative to the

CT strain ($0.262 \pm 0.080\,day^{-1}$), consistent with it having a higher $T_{min}$ (14.94 vs. 0.02°C for CT; Table S1). It also downregulated considerably more transcripts and functions (2008 transcripts within 27 enriched BP GO categories compared with 94 transcripts and 7 enriched BP GO categories in CT; Figure 5a, Figure S1), including 26 transcripts pertaining to the photosynthetic light harvesting complex (chlorophyll A–B binding proteins) (Figure 5b). DNA repair enzymes and HSPs and related chaperones were also encoded among the downregulated transcripts in the HT strain at 21°C (25–4°C) (Figure 5C), suggesting a broad-scale shift in metabolism. In the upwards phase of each temperature regime, all strains were actively dividing, despite being exposed to absolute temperatures approaching their thermal maximum ($T_{max}$) (Table S1). Under periodic exposure to 34°C (upwards phase of 30 + 4°C for *Amphidinium* only), both the HT and CT *A. massartii* strains showed a large number of differentially expressed transcripts relative to the 30°C stable mean control (2523 and 3374 for HT and CT, respectively), with the majority of those transcripts upregulated at 34°C (78% and 76% for HT and CT, respectively) (Figure S1). In both *Amphidinium* strains, transcripts encoding functions involved in DNA recombination and integration were enriched in the upregulated transcripts, indicative of genomic changes at 34°C (Figure S4).

Together, these observations suggest that variable temperatures approaching upper thermal limits led to increased metabolism, despite contrasting effects on growth, and that in fluctuating environments, cells may tolerate periodic exposure to temperature extremes with limited signs of stress.

## 4 | DISCUSSION

A greater understanding of the consequences of thermal variation are needed to make predictions about the current and future growth, abundance, and distributions of species in the natural environment. Climate change models not only forecast higher mean temperatures in the future ocean but also that the magnitude, frequency, and extremes of temperature variability will increase (Boyd et al., 2016; Frölicher et al., 2018; IPCC, 2014, 2018; Thornton et al., 2014; Vasseur et al., 2014). Here we show that regular 2-day temperature fluctuations of the type often observed in coastal waters (AIMS, 2009; Dai et al., 2009; Leinweber et al., 2009; Shaw et al., 2012), can cause significant demographic and biogeochemical impacts on microbial eukaryotes, and that phenotypic trait values diverge at a similar absolute temperature depending on previous

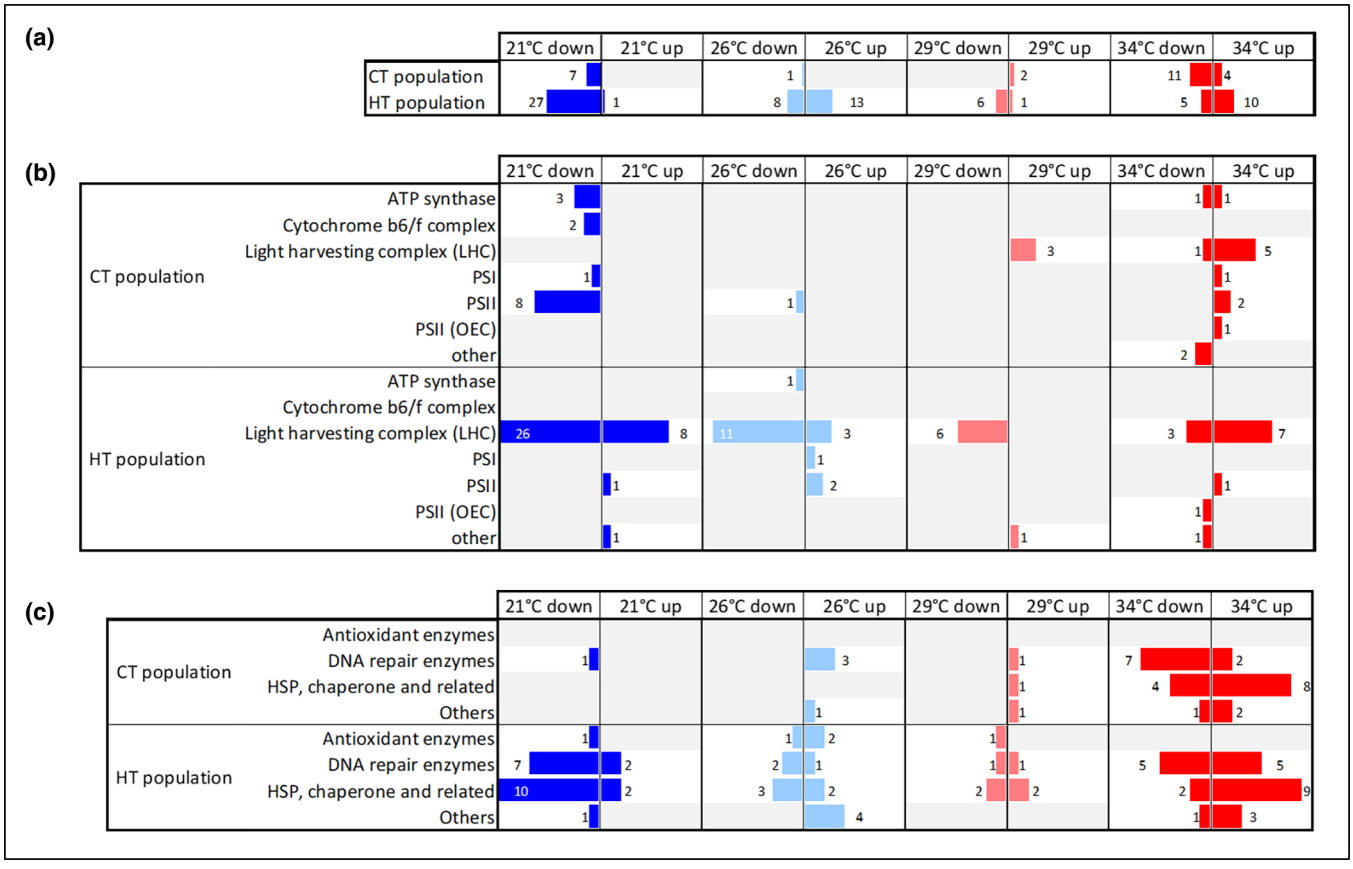


FIGURE 5 Transcriptional plasticity of dinoflagellates. Number of biological process gene ontology categories enriched in differentially expressed transcripts (a), differentially expressed transcripts encoding photosynthesis (b) and stress functions (c) for *A. massartii* control temperature and high-temperature strains growing at fluctuating temperatures (25°C ± 4 (21 and 29) and 30°C ± 4 (26 and 34)) relative to stable controls. "down/up" refers to downregulated and upregulated differentially expressed transcripts, respectively.

thermal history. Furthermore, the existence of *Response D* (decline in growth under both upwards and downwards shifts in temperature from a supra-optimal mean) indicates that predicting responses is not as straight forward as understanding the shape of TPCs.

Our expectation was that average population growth rates would decrease under variable temperature treatments because cells spent less time within their $T_{opt}$ range, and that the decline would be proportional to the amplitude of temperature fluctuation because increasingly variable regimes impose an energetic cost (Putnam & Edmunds, 2011). Given that TPCs are non-linear (Huey & Stevenson, 1979), with an accelerating phase of growth at temperatures below $T_{opt}$ and a decelerating phase of growth at temperatures greater than $T_{opt}$, we anticipated *Response A*, where instantaneous growth rates decreased during the downward phase and increased during the upwards phase of fluctuations (Bernhardt et al., 2018). However, there was a net loss of fitness when temperature fluctuated around a supra-optimal mean, as demonstrated by the non-reversibility of growth (i.e., *Response D*) in temperate *C. malayensis* and *A. massartii* CT and HT—that is, no increase in growth rate during the downward phase as temperature approached $T_{opt}$. This indicates there is an interaction between temperature variability and mean temperature that fundamentally alters cellular processes, with cascading effects on growth and phenotypic traits. One direction for future work would be to determine the threshold temperature above $T_{opt}$ and associated fluctuations where phenotypic responses are no longer reversible, and what other factors affect the temperature at which this thermal tipping point occurs.

Although there is well-established theory that overall phenotypic plasticity increases when populations evolve in predictably variable environments, and some empirical evidence that environmental fluctuations with fixed period but random amplitude select for plastic individuals (Botero et al., 2015; Lande, 2009; Schaum et al., 2016), the combinations of traits that phytoplankton use to increase plasticity is less well known. The elemental content of C, N, and P was proportional to cell volume which flexed depending on growth rate at temperatures below $T_{opt}$, demonstrating its utility as a "master trait" (Litchman & Klausmeier, 2008). Given that C, N, and P make up most microbial biomass (Finkel et al., 2016), changes in these traits with cell size were expected. However, pigment content and GPP were not related to cell size, and at temperature extremes it was evident that fixed carbon was being redirected into non-growth components—for example, respiration or dissolved organic carbon release or both. Our observations also showed that the *A. massartii* HT strain diverged from its CT descendant, showing higher N content than at the stable mean temperature of 30°C, consistent with its increased N demand associated with its high-temperature adaptation (Baker et al., 2018). Furthermore, C:N and N:P ratios were related to cell volume but showed contrasting patterns in *Amphidinium* versus *Coolia*. There was also a common pattern of increasing heterogeneity among phenotypes at temperatures exceeding $T_{opt}$. Although many ocean biogeochemical models include correlations between traits (e.g., those that incorporate flexible C:N:P stoichiometry), many overlook how these correlations may change with adaptation to climate change. Collapsing multi-trait phenotypes, derived from experiments such as this, into two dimensions using multi-variate methods may provide a pathway for integrating plasticity and evolution into ocean biogeochemical models (Argyle et al., 2021; Walworth et al., 2021).

Another aspect of plasticity revealed by transcriptomic analyses in this study was that microbial eukaryotes can be in physiologically different states while exhibiting similar growth rates. The ability to down- and up-regulate metabolism whilst maintaining a consistent growth rate was demonstrated by the tropical *C. palmyrensis* strain fluctuating between 21 and 29°C (25 ± 4°C; Figure 2 and Figure S4). Alternatively, broadscale downregulation may be a conservative strategy that protects cells against damage when approaching temperature limits (Kültz, 2005) but requires cells to rapidly respond to changes in their external conditions. The response of *C. palmyrensis* to the sub-optimal temperature at 16°C (downward phase of 20 ± 4°C) involved cell persistence and cessation of cell division (Figure 2), but no major restructuring of metabolism (Figures S3 and S4). Importantly, our gene expression analyses showed that temperatures of upper and lower thermal growth limits determined under stable conditions (Table S1) were not necessarily stress-inducing or fatal for cells that only periodically experienced these extreme temperatures. Temporary respite from high or low temperature evidently allowed populations to limit cumulative stress, as was shown by Schaum et al. (2018) for a marine diatom in fluctuating temperature regimes. These observations are in line with field data that show similar composition of dinoflagellates within phytoplankton communities in the tropical Pacific Ocean despite a clear environmental gradient in temperature and nutrient limitation (Cohen et al., 2021), suggesting that regulation of gene expression is critical to plasticity in situ. However, thermal tolerance within any single taxon could be surpassed during marine heatwaves (temperatures above a seasonally varying 90th percentile for at least 5 days at a particular location; Hobday et al., 2018). Indeed, in mixed natural phytoplankton communities from the San Pedro Ocean Time-series station exposed to mean temperatures that exceeded multiyear upper thermal limits and fluctuated ±4°C, there was a complete restructuring of the community (Kling et al., 2020).

At the outset of this study, we hypothesised that the thermal histories (i.e., differing isolation locations or laboratory selection regimes) and higher $T_{opt}$ of *A. massartii* HT and tropical *C. palmyrensis* would lead to greater vulnerability to temperature variability. However, this was not the case, with narrower thermal niche breadth the common factor among strains that had the most detrimental impacts to growth under fluctuating temperature.

The mean temperatures used in our experiments were 20, 25, and 30°C, representative of temperate, sub-tropical and tropical ocean waters, respectively, and therefore relevant to species growing in a large proportion of the global ocean (Locarnini et al., 2018). Fluctuation regimes were designed to have regular intervals (2 days) that would not be biologically anticipated through diel light cues (Ottesen et al., 2014; Vislova et al., 2019). In general, *A. massartii* populations were more responsive to temperature shifts, moderating

growth rates up and down when temperatures fluctuated. Given that fluctuations occurred every 2 days, this exposed *Amphidinium* cells to temperatures that allowed for cell division, whereas for *Coolia* spp., temperature exposures were within a single generation. This suggests that different generational times could set the pace of acclimatization relative to the frequency of environmental change—that is, fast-growing taxa with short generation times could potentially alter their cell physiology at similar time scales to environmental fluctuations. Among freshwater phytoplankton taxa Fey et al. (2021) found greater support for gradual thermal acclimation that lagged behind changes in temperature, rather than instantaneous adjustments. Furthermore, mechanisms such as nutrient storage could allow large cells to "ride out" changes in the external environment. Considering that growth rates are intrinsically related to cell size (Litchman et al., 2007), our results potentially provide a unifying framework with which to test the implications of environmental fluctuations on microbial taxa spanning orders of magnitude in size.

## 5 | CONCLUSION

With the ocean projected to become warmer and more variable, investigations that connect aspects of environmental variation with organismal plasticity and evolution are urgently needed (Collins et al., 2020). Here we show clear evidence that microbial eukaryotes diverge in their responses to temperature fluctuations depending on whether mean temperature is above or below $T_{opt}$, with the magnitude of impact being mediated by their degree of thermal specialisation. Our selection of strains allowed comparison of dinoflagellate taxa with similar thermal traits isolated from different latitudes (*Coolia* spp.) as well as a comparison of strains from the same ancestor that were maintained at different temperatures (*A. massartii*), both of which showed clear differences linked to narrower thermal niche breadth not $T_{opt}$ as we hypothesised. The implications are that species with narrower TPCs under a warming baseline could be more vulnerable to changes in temperature variation, with cascading impacts to global biogeochemical cycles and climate feedbacks.

### FUNDING INFORMATION

This research was funded by the Australian Government through the Australian Research Council Discovery Scheme (project no. DP140101340 awarded to MD, SM, and DH and DP180100054 awarded to MD). FF and DH were funded by a University of Technology Sydney Distinguished Visiting Professor Scheme. Additional support was provided by U.S. National Science Foundation grant OCE 1638804 to DH and OCE 1851222 to FF and DH. KB, ML were each supported by an Australian Government Training Program Scholarship.

### ACKNOWLEDGEMENT

Open access publishing facilitated by University of Technology Sydney, as part of the Wiley - University of Technology Sydney agreement via the Council of Australian University Librarians.

### CONFLICT OF INTEREST

MD is a member of the board of directors for the Sydney Institute of Marine Science.

### DATA AVAILABILITY STATEMENT

Raw sequencing data has been deposited to the NCBI Sequence Read Archive under Bioproject PRJNA819215. Additional data is available on Dryad at https://doi.org/10.5061/dryad.xd2547dkq

### ORCID

*Bernhard Tschitschko* https://orcid.org/0000-0002-0379-3187
*David A. Hutchins* https://orcid.org/0000-0002-6637-756X
*Martina A. Doblin* https://orcid.org/0000-0001-8750-3433

### REFERENCES

Aguirre, C., Garreaud, R., Belmar, L., Farías, L., Ramajo, L., & Barrera, F. (2021). High-frequency variability of the surface ocean properties off central chile during the upwelling season. *Frontiers in Marine Science*, *8*. https://doi.org/10.3389/fmars.2021.702051

Araújo, M. B., Pearson, R. G., Thuiller, W., & Erhard, M. (2005). Validation of species–climate impact models under climate change. *Global Change Biology*, *11*, 1–10.

Argyle, P. A., Walworth, N. G., Hinners, J., Collins, S., Levine, N. M., & Doblin, M. A. (2021). Multivariate trait analysis reveals diatom plasticity constrained to a reduced set of biological axes. *ISME Communications*, *1*. https://doi.org/10.1038/s43705-021-00062-8

Arias, P. A., Bellouin, N., Coppola, E., Jones, R. G., Krinner, G., Marotzke, J., Naik, V., Palmer, M. D., Plattner, G.-K., Rogelj, J., Rojas, M., Sillmann, J., Storelvmo, T., Thorne, P. W., Trewin, B., Rao, K. A., Adhikary, B., Allan, R. P., Armour, K., … Zickfeld, K. (2021). Technical summary. In V. Masson-Delmotte, P. Zhai, A. Pirani, S. L. Connors, C. Péan, S. Berger, N. Caud, Y. Chen, L. Goldfarb, M. I. Gomis, M. Huang, K. Leitzell, E. Lonnoy, J. B. R. Matthews, T. K. Maycock, T. Waterfield, O. Yelekçi, R. Yu, & B. Zhou (Eds.), *Climate change 2021: The physical science basis. Contribution of Working Group I to the Sixth Assessment Report of the Intergovernmental Panel on Climate Change* (pp. 33–144). Cambridge University Press. https://doi.org/10.1017/9781009157896.002

Australian Institute of Marine Science (AIMS). (2009). *Northern Australia automated marine weather and oceanographic stations* https://doi.org/10.25845/5c09bf93f315d

Baker, K. G., Radford, D. T., Evenhuis, C., Kuzhiumparam, U., Ralph, P. J., & Doblin, M. A. (2018). Thermal niche evolution of functional traits in a tropical marine phototroph. *Journal of Phycology*, *56*, 799–810.

Baker, K. G., Robinson, C. M., Radford, D. T., McInnes, A. S., Evenhuis, C., & Doblin, M. A. (2016). Thermal performance curves of functional traits aid understanding of thermally induced changes in diatom-mediated biogeochemical fluxes. *Frontiers in Marine Science*, *3*, 44. https://doi.org/10.3389/fmars.2016.00044

Benjamini, Y., & Yosef, H. (1995). Controlling the false discovery rate: A practical and powerful approach to multiple testing. *Journal of the Royal Statistical Society. Series B (Methodological)*, *57*(1), 289–300. http://www.jstor.org/stable/2346101

Bernhardt, J. R., Sunday, J. M., Thompson, P. L., & O'Connor, M. I. (2018). Nonlinear averaging of thermal experience predicts population growth rates in a thermally variable environment. *Proceedings of the Royal Society B*, *285*, 20181076. https://doi.org/10.1098/rspb.2018.1076

Bolger, A. M., Lohse, M., & Usadel, B. (2014). Trimmomatic: A flexible trimmer for Illumina sequence data. *Bioinformatics*, *30*(15), 2114–2120. https://doi.org/10.1093/bioinformatics/btu170

Botero, C. A., Weissing, F. J., Wright, J., & Rubenstein, D. R. (2015). Evolutionary tipping points in the capacity to adapt to environmental change. *PNAS*, *112*, 184–189.

Boyd, P. W., Cornwall, C. E., Davison, A., Doney, S. C., Fourquez, M., Hurd, C. L., Lima, I. D., & McMinn, A. (2016). Biological responses to environmental heterogeneity under future ocean conditions. *Global Change Biology*, *22*(8), 2633–2650. https://doi.org/10.1111/gcb.13287

Bray, N. L., Pimentel, H., Melsted, P., & Pachter, L. (2016). Near-optimal probabilistic RNA-seq quantification. *Nature Biotechnology*, *34*(5), 525–527. https://doi.org/10.1038/nbt.3519

Cabrerizo, M. J., Marañón, E., Fernández-González, C., Alonso-Núñez, A., Larsson, H., & Aranguren-Gassis, M. (2021). Temperature fluctuation attenuates the effects of warming in estuarine microbial plankton communities. *Frontiers in Marine Science*, *8*, 656282. https://doi.org/10.3389/fmars.2021.656282

Camacho, C., Coulouris, G., Avagyan, V., Ma, N., Papadopoulos, J., & Bealer, K., & Madden, T. L. BLAST+: Architecture and applications. *BMC Bioinformatics* 2009 *15*;10:421. doi: https://doi.org/10.1186/1471-2105-10-421. PMID: 20003500; PMCID: PMC2803857

Cohen, N. R., McIlvin, M. R., Moran, D. M., Held, N. A., Saunders, J. K., Hawco, N. J., Brosnahan, M., DiTullio, G. R., Lamborg, C., McCrow, J. P., Dupont, C. L., Allen, A. E., & Saito, M. A. (2021). Dinoflagellates alter their carbon and nutrient metabolic strategies across environmental gradients in the central Pacific Ocean. *Nature Microbiology*, *6*, 173–186.

Collins, S., Boyd, P. W., & Doblin, M. A. (2020). Evolution, microbes, and changing ocean conditions. *Annual Review of Marine Science*, *12*, 181–208.

Dai, M., Lu, Z., Zhai, W., Chen, B., Cao, Z., Zhou, K., Cai, W., & Chen, C. A. (2009). Diurnal variations of surface seawater $pCO_2$ in contrasting coastal environments. *Limnology and Oceanography*, *54*, 735–745.

Daufresne, M., Lengfellner, K., & Sommer, U. (2009). Global warming benefits the small in aquatic ecosystems. *Proceedings of the National Academy of Sciences of the United States of America*, *106*, 12788–12793.

Doblin, M. A., Ralph, P. J., Petrou, K. L., Shelly, K., Westwood, K., van den Enden, R., Wright, S., & Griffiths, B. (2011). Diel variation of chl-a fluorescence, phytoplankton pigments and productivity in the Sub-Antarctic Zone. *Deep Sea Research II: Topical Studies in Oceanography*, *58*(21–22), 2189–2199.

Doblin, M. A., & van Sebille, E. (2016). Drift in ocean currents impacts intergenerational microbial exposure to temperature. *Proceedings of the National Academy of Sciences of the United States of America*, *113*, 5700–5705.

Domingues, C. M., Church, J. A., White, N. J., Gleckler, P. J., Wijffels, S. E., Barker, P. M., & Dunn, J. R. (2008). Improved estimates of upper-ocean warming and multi-decadal sea level rise. *Nature*, *453*, 1090–1093. https://doi.org/10.1038/nature07080

Dutkiewicz, S., Morris, J. J., Follows, M. J., Scott, J., Levitan, O., Dyhrman, S. T., & Berman-Frank, I. (2015). Impact of ocean acidification on the structure of future phytoplankton communities. *Nature Climate Change*, *5*, 1002–1006.

Dutkiewicz, S., Scott, J. R., & Follows, M. J. (2013). Winners and losers: Ecological and biogeochemical changes in a warming ocean. *Global Biogeochemical Cycles*, *27*, 463–477. https://doi.org/10.1002/gbc.20042

Eppley, R. W. (1972). Temperature and phytoplankton growth in the sea. *Fishery Bulletin*, *70*, 1063–1085.

Feder, M. E., & Hofmann, G. E. (1999). Heat-shock proteins, molecular chaperones, and the stress response: Evolutionary and ecological physiology. *Annual Review of Physiology*, *61*, 243–282. https://doi.org/10.1146/annurev.physiol.61.1.243

Fey, S. B., Kremer, C. T., Layden, T. J., & Vasseur, D. A. (2021). Resolving the consequences of gradual phenotypic plasticity for populations in variable environments. *Ecological Monographs*, *91*(4), e01478. https://doi.org/10.1002/ecm.1478

Finkel, Z. V., Follows, M. J., Liefer, J. D., Brown, C. M., Benner, I., & Irwin, A. J. (2016). Phylogenetic diversity in the macromolecular composition of microalgae. *PLoS ONE*, *11*(5), e0155977. https://doi.org/10.1371/journal.pone.0155977

Frölicher, T. L., Fischer, E. M., & Gruber, N. (2018). Marine heatwaves under global warming. *Nature*, *560*, 360–364.

Fu, F. X., Zhang, Y., Leblanc, K., Sañudo-Wilhelmy, S. A., & Hutchins, D. A. (2005). The biological and biogeochemical consequences of phosphate scavenging onto phytoplankton cell surfaces. *Limnology and Oceanography*, *50*, 1459–1472.

Garcia-Soto, C., Cheng, L., Caesar, L., Schmidtko, S., Jewett, E. B., Cheripka, A., Rigor, I., Caballero, A., Chiba, S., Báez, J. C., Zielinski, T., & Abraham, J. P. (2021). An overview of ocean climate change indicators: Sea surface temperature, ocean heat content, ocean pH, dissolved oxygen concentration, arctic sea ice extent, thickness and volume, sea level and strength of the AMOC (Atlantic Meridional Overturning Circulation). *Frontiers in Marine Science*, *8*, 642372. https://doi.org/10.3389/fmars.2021.642372

Gill, R. L., Collins, S., Argyle, P. A., Larsson, M. E., Fleck, R., & Doblin, M. A. (2022). Predictability of thermal fluctuations influences functional traits of a cosmopolitan marine diatom. *Proceedings of the Royal Society B*, *289*, 20212581. https://doi.org/10.1098/rspb.2021.2581

Gotz, S., Garcia-Gomez, J. M., Terol, J., Williams, T. D., Nagaraj, S. H., Nueda, M. J., Robles, M., Talon, M., Dopazo, J., & Conesa, A. (2008). High-throughput functional annotation and data mining with the Blast2GO suite. *Nucleic Acids Research*, *36*(10), 3420–3435. https://doi.org/10.1093/nar/gkn176

Grabherr, M. G., Haas, B. J., Yassour, M., Levin, J. Z., Thompson, D. A., Amit, I., Adiconis, X., Fan, L., Raychowdhury, R., Zeng, Q., Chen, Z., Mauceli, E., Hacohen, N., Gnirke, A., Rhind, N., di Palma, F., Birren, B. W., Nusbaum, C., Lindblad-Toh, K., … Regev, A. (2011). Full-length transcriptome assembly from RNA-Seq data without a reference genome. *Nature Biotechnology*, *29*(7), 644–652. https://doi.org/10.1038/nbt.1883

Guillard, R. R., & Ryther, J. H. (1962). Studies of marine planktonic diatoms.I. Cyclothellanana Hustedt and Detonula *confervacea* Gran. *Canadian Journal of Microbiology*, *8*, 229–239. https://doi.org/10.1139/m62-029

Haas, B. J., Papanicolaou, A., Yassour, M., Grabherr, M., Blood, P. D., Bowden, J., Couger, M. B., Eccles, D., Li, B., Lieber, M., Macmanes, M. D., Ott, M., Orvis, J., Pochet, N., Strozzi, F., Weeks, N., Westerman, R., William, T., Dewey, C. N., … Regev, A. (2013). De novo transcript sequence reconstruction from RNA-seq using the Trinity platform for reference generation and analysis. *Nature Protocols*, *8*(8), 1494–1512. https://doi.org/10.1038/nprot.2013.084

Hillebrand, H., Dürselen, C., Kirschtel, D., Pollingher, U., & Zohary, T. (1999). Biovolume calculation for pelagic and benthic microalgae. *Journal of Phycology*, *35*, 403–424.

Hobday, A. J., Oliver, E. C. J., Sen Gupta, A., Benthuysen, J. A., Burrows, M. T., Donat, M. G., Holbrook, N. J., Moore, P. J., Thomsen, M. S., Wernberg, T., & Smale, D. A. (2018). Categorizing and naming marine heatwaves. *Oceanography*, *31*, 162–173.

Huey, R. B., & Stevenson, R. D. (1979). Integrating thermal physiology and ecology of ectotherms: A discussion of approaches. *American Zoologist*, *19*, 357–366.

Hutchins, D. A., DiTullio, G. R., Zhang, Y., & Bruland, K. W. (1998). An iron limitation mosaic in the California coastal upwelling regime. *Limnology and Oceanography*, *43*, 1037–1054.

IPCC. (2014). Climate change 2014: Synthesis report. In Core Writing Team, R. K. Pachauri, & L. A. Meyer (Eds.), *Contribution of Working Groups I, II and III to the Fifth Assessment Report of the Intergovernmental Panel on Climate Change* (p. 151). IPCC.

IPCC. (2018). Summary for policymakers. In V. Masson-Delmotte, P. Zhai, H. O. Pörtner, D. Roberts, J. Skea, P. R. Shukla, A. Pirani, W. Moufouma-Okia, C. Péan, R. Pidcock, S. Connors, J. B. R. Matthews, Y. Chen, X. Zhou, M. I. Gomis, E. Lonnoy, T. Maycock, M. Tignor, & T. Waterfield (Eds.), *Global warming of 1.5°C. An IPCC Special Report on the impacts of global warming of 1.5°C above pre-industrial levels and related global greenhouse gas emission pathways, in the context of strengthening the global response to the threat of climate change, sustainable development, and efforts to eradicate poverty* (p. 32). World Meteorological Organization.

Jones, P., Binns, D., Chang, H. Y., Fraser, M., Li, W., McAnulla, C., McWilliam, H., Maslen, J., Mitchell, A., Nuka, G., Pesseat, S., Quinn, A. F., Sangrador-Vegas, A., Scheremetjew, M., Yong, S. Y., Lopez, R., & Hunter, S. (2014). InterProScan 5: Genome-scale protein function classification. *Bioinformatics*, *30*(9), 1236–1240. https://doi.org/10.1093/bioinformatics/btu031

Kling, J. D., Lee, M. D., Fu, F., Phan, M. D., Wang, X., Qu, P., & Hutchins, D. A. (2020). Transient exposure to novel high temperatures reshapes coastal phytoplankton communities. *The ISME Journal*, *14*, 413–424.

Kroeker, K. J., Bell, L. E., Donham, E. M., Hoshijima, U., Lummis, S., Toy, J. A., & Willis-Norton, E. (2020). Ecological change in dynamic environments: Accounting for temporal environmental variability in studies of ocean change biology. *Global Change Biology*, *26*, 54–67.

Kültz, D. (2005). Molecular and evolutionary basis of the cellular stress response. *Annual Review of Physiology*, *67*, 225–257.

Lande, R. (2009). Adaptation to an extraordinary environment by evolution of phenotypic plasticity and genetic assimilation. *Journal of Evolutionary Biology*, *22*, 1435–1446.

Larsson, M. E., Smith, K., & Doblin, M. A. (2019). First description of the environmental niche of the epibenthic dinoflagellates *Coolia palmyrensis*, *C. malayensis* and *C. tropicalis* (Dinophyceae) from eastern Australia. *Journal of Phycology*, *55*, 565–577.

Leinweber, A., Gruber, N., Frenzel, H., & Chavez, F. P. (2009). Diurnal carbon cycling in the surface ocean and lower atmosphere of Santa Monica Bay, California. *Geophysical Research Letters*, *36*, L08601.

Leung, C., Rescan, M., Grulois, D., & Chevin, L. (2020). Reduced phenotypic plasticity evolves in less predictable environments. *Ecology Letters*, *23*, 1664–1672.

Litaker, R. W., Vandersea, M. W., Faust, M. A., Kibler, S. R., Chinain, M., Holmes, M. J., Holland, W. C., & Tester, P. A. (2009). Taxonomy of *Gambierdiscus* including four new species, *Gambierdiscus caribaeus*, *Gambierdiscus carolinianus*, *Gambierdiscus carpenteri* and *Gambierdiscus ruetzleri* (Gonyaulacales, Dinophyceae). *Phycologia*, *48*, 344–390.

Litchman, E., & Klausmeier, C. A. (2008). Trait-based community ecology of phytoplankton. *Annual Review of Ecology, Evolution, and Systematics*, *39*, 615–639.

Litchman, E., Klausmeier, C. A., Schofield, O. M., & Falkowski, P. G. (2007). The role of functional traits and trade-offs in structuring phytoplankton communities: Scaling from cellular to ecosystem level. *Ecology Letters*, *10*, 1170–1181.

Locarnini, R. A., Mishonov, A. V., Baranova, O. K., Boyer, T. P., Zweng, M. M., Garcia, H. E., Reagan, J. R., Seidov, D., Weathers, K., Paver, C. R., & Smolyar, I.. (2018). World Ocean Atlas 2018, Volume 1: Temperature. A. Mishonov Technical Ed.; NOAA Atlas NESDIS 81, 52 pp.

Marie, D., Partensky, F., Vaulot, D., & Brussaard, C. (1999). Enumeration of phytoplankton, bacteria, and viruses in marine samples. *Current Protocols in Cytometry*, *11*(11), s.

Murray, S. A., Garby, T., Hoppenrath, M., & Neilan, B. A. (2012). Genetic diversity, morphological uniformity and polyketide production in dinoflagellates (*Amphidinium*, Dinoflagellata). *PLoS One*, *7*(6), e38253.

Oliver, E. C. J., Donat, M. G., Burrows, M. T., Moore, P. J., Smale, D. A., Alexander, L. V., Benthuysen, J. A., Feng, M., Sen Gupta, A., Hobday, A. J., Holbrook, N. J., Perkins-Kirkpatrick, S. E., Scannell, H. A., Straub, S. C., & Wernberg, T. (2018). Longer and more frequent marine heatwaves over the past century. *Nature Communications*, *9*, 1324.

Ottesen, E. A., Young, C. R., Gifford, S. M., Eppley, J. M., Marin, R., Schuster, S. C., Scholin, C. A., & DeLong, E. F. (2014). Multispecies diel transcriptional oscillations in open ocean heterotrophic bacterial assemblages. *Science*, *345*(6193), 207–212.

Pansch, C., & Hiebenthal, C. (2019). A new mesocosm system to study the effects of environmental variability on marine species and communities. *Limnology and Oceanography*, *17*, 145–162.

Putnam, H. M., & Edmunds, P. J. (2011). The physiological response of reef corals to diel fluctuations in seawater temperature. *Journal of Experimental Marine Biology and Ecology*, *396*(2011), 216–223.

Qu, P., Fu, F.-X., Kling, J., Huh, M., Wang, X., & Hutchins, D. A. (2019). Distinct responses of *Trichodesmium* to a thermally-variable environment as a function of phosphorus availability. *Frontiers in Microbiology*, *10*, 1282. https://doi.org/10.3389/fmicb.2019.01282

Robinson, M. D., McCarthy, D. J., & Smyth, G. K. (2010). edgeR: A Bioconductor package for differential expression analysis of digital gene expression data. *Bioinformatics*, *26*(1), 139–140. https://doi.org/10.1093/bioinformatics/btp616

Schaum, E., Buckling, A., Smirnoff, N., Studholme, D. J., & Yvon-Durocher, G. (2018). Environmental fluctuations accelerate molecular evolution of thermal tolerance in a marine diatom. *Nature Communications*, *9*, 1719–1732.

Schaum, E., Rost, B., & Collins, S. (2016). Environmental stability affects phenotypic evolution in a globally distributed marine picoplankton. *The ISME Journal*, *10*, 75–84.

Schlichting, C., & Pigliucci, M. (1998). *Phenotypic evolution: A reaction norm perspective* (p. 387). Sinauer Associates Inc.

Shaw, E. C., McNeil, B. I., & Tilbrook, B. (2012). Impacts of ocean acidification in naturally variable coral reef flat ecosystems. *Journal of Geophysical Research: Oceans*, *117*, C03038. https://doi.org/10.1029/2011JC007655

Simão, F. A., Waterhouse, R. M., Ioannidis, P., Kriventseva, E. V., & Zdobnov, E. M. (2015). BUSCO: Assessing genome assembly and annotation completeness with single-copy orthologs. *Bioinformatics*, *31*(19), 3210–3212. https://doi.org/10.1093/bioinformatics/btv351

Strickland, J. D. H., & Parsons, T. R. (1968). *A practical handbook of seawater analysis* (p. 167.311). Fisheries Research Board of Canada Bulletin.

Thomas, M. K., Kremer, C. T., Klausmeier, C. A., & Litchman, E. (2012). A global pattern of thermal adaptation in marine phytoplankton. *Science*, *338*, 1085–1088.

Thornton, P. K., Ericksen, P. J., Herrero, M., & Challinor, A. J. (2014). Climate variability and vulnerability to climate change: A review. *Global Change Biology*, *20*(11), 3313–3328. https://doi.org/10.1111/gcb.12581

Toseland, A., Daines, S. J., Clark, J. R., Kirkham, A., Strauss, J., Uhlig, C., Lenton, T. M., Valentin, K., Pearson, G. A., Moulton, V., & Mock, T. (2013). The impact of temperature on marine phytoplankton resource allocation and metabolism. *Nature Climate Change*, *3*, 979–984.

Valentin, K., & Mock, T. (2004). Photosynthesis and cold acclimation: Molecular evidence from a polar diatom. *Journal of Phycology*, *40*, 732–741.

Vasseur, D. A., Delong, J. P., Gilbert, B., Greig, H. S., Harley, C. D. G., McCann, K. S., Savage, V., Tunney, T. D., & O'Connor, M. I. (2014). Increased temperature variation poses a greater risk to species than climate warming. *Proceedings of the Royal Society B*, *281*, 20132612.

Verma, A., Kohli, G. S., Harwood, D. T., Ralph, P. J., & Murray, S. A. (2019). Transcriptomic investigation into polyketide toxin synthesis in Ostreopsis (Dinophyceae) species. *Environmental Microbiology*, *21*(11), 4196–4211. https://doi.org/10.1111/1462-2920.14780

Vislova, A., Sosa, O. A., Eppley, J. M., Romano, A. E., & DeLong, E. F. (2019). Diel oscillation of microbial gene transcripts declines with depth in oligotrophic ocean waters. *Frontiers in Microbiology*, *10*, 2191. https://doi.org/10.3389/fmicb.2019.02191

Walworth, N. G., Hinners, J., Argyle, P. A., Leles, S. G., Doblin, M. A., Collins, S., & Levine, N. M. (2021). The evolution of trait correlations constrains phenotypic adaptation to high $CO_2$ in a eukaryotic alga. *Proceedings of the Royal Society B*, *288*, 20210940.

Weizhong, L., & Adam, G. (2006). Cd-hit: A fast program for clustering and comparing large sets of protein or nucleotide sequences. *Bioinformatics*, *22*, 1658–1659.

Woods, H. A., Makino, W., Cotner, J. B., Hobbie, S. E., Harrison, J. F., Acharya, K., & Elser, J. J. (2003). Temperature and the chemical composition of poikilothermic organisms. *Functional Ecology*, *17*, 237–245.

## SUPPORTING INFORMATION

Additional supporting information can be found online in the Supporting Information section at the end of this article.

**How to cite this article:** Fu, F.-X., Tschitschko, B., Hutchins, D. A., Larsson, M. E., Baker, K. G., McInnes, A., Kahlke, T., Verma, A., Murray, S. A., & Doblin, M. A. (2022). Temperature variability interacts with mean temperature to influence the predictability of microbial phenotypes. *Global Change Biology*, *28*, 5741–5754. https://doi.org/10.1111/gcb.16330